JEE Journal of Ecological Engineering

Journal of Ecological Engineering, 2027, 28(1), 207–231
https://doi.org/10.12911/22998993/241836
ISSN 2299–8993, License CC-BY 4.0

Received: 2026.09.01
Accepted: 2026.11.16
Published: 2026.12.01

Scenario-based hydraulic resilience assessment and sensitivity-based monitoring framework for a gravity-based water distribution network: A case study in Al-Salt, Jordan

Omar A. Ahmad[1*], A. Assi[1], M. Abufarah[1], M. Awad[1], Y. Abu Saleem[1]

[1] Department of Civil Engineering, College of Engineering, Amman Arab University, 11953 Amman, Jordan
* Corresponding author's e-mail: oahmad@aau.edu.jo

ABSTRACT

Increasing water scarcity, urban growth, and operational uncertainty require water infrastructure systems capable of maintaining acceptable hydraulic performance under changing conditions. This study develops a scenario-based resilience assessment and hydraulic sensitivity-based monitoring framework for a gravity-based water distribution network using Naqab Al-Dabur, Al-Salt, Jordan, as a case study. The system serves approximately 5.000 inhabitants across 135 multi-family residential buildings and operates using an available elevation difference of approximately 53 m. An independently developed steady-state hydraulic model was established using Bentley WaterGEMS design information and validated against the exported Bentley WaterGEMS baseline solution. The validated model was applied to assess baseline (1.00×), future-growth (1.20×), maximum-day (1.50×), peak-demand-equivalent (2.00×), and single-pipe outage scenarios. The baseline model represented an assigned demand of 501.55 m³/day. Increasing hydraulic loading progressively reduced pressure margins, with minimum pressure decreasing from 2.44 bar under baseline conditions to 1.46 bar under peak-demand-equivalent loading. Junctions J-41 and J-116 were identified as demand-sensitive locations because their pressures decreased below the 1.5-bar service-pressure criterion. Pipe velocity increased from 0.71 m/s to 1.42 m/s, with PIP-3 representing the primary hydraulic loading pathway. Single-pipe outage analysis revealed greater localized vulnerability; removal of PIP-30 reduced minimum residual pressure to −1.06 bar at J-34, affected 21 junctions, and increased rerouted velocity in PIP-2 to 1.55 m/s. Fourteen bridge-link pipes were identified as topologically critical components due to their connectivity impacts. The hydraulic sensitivity results were translated into a system-specific monitoring framework by linking priority locations with pressure, flow, velocity, and asset-status indicators. The proposed approach demonstrates how scenario-based hydraulic analysis can support targeted monitoring design and improve operational awareness in gravity-based water distribution networks.

Keywords: hydraulic resilience, scenario-based modelling, gravity-based water distribution system, hydraulic sensitivity analysis, monitoring framework, water distribution network management.

INTRODUCTION

Water distribution networks are critical urban infrastructure systems that support public health, environmental protection, and socioeconomic development. However, population growth, urban expansion, changing consumption patterns, and climate-related uncertainty increasingly challenge the ability of water systems to maintain reliable hydraulic performance under variable operating conditions (Di Nardo et al., 2021; Krishnan et al., 2022). These challenges are particularly important in water-scarce regions, where maintaining service reliability requires improved understanding of network behaviour under changing hydraulic conditions (Maroju et al., 2023). In Jordan, improving water and energy efficiency remains an important sustainability priority due to increasing demand pressures and limited water resources (Alwidyan et al., 2026).

Gravity-based water distribution systems provide an opportunity to reduce pumping requirements and operational complexity by utilizing available elevation differences to generate hydraulic head. However, satisfactory performance under a single design condition does not necessarily ensure resilience under future demand increases or localized disturbances. Variations in demand, network loading, and component availability can modify pressure distribution, flow behaviour, and service reliability, requiring evaluation beyond conventional design-state analysis.

Hydraulic modelling remains a fundamental approach for evaluating water distribution system performance by representing pressure distribution, flow behaviour, and operational response under different conditions (Walski et al., 2003; Rossman, 2022). Recent developments have extended hydraulic models toward more integrated operational applications by connecting infrastructure models with data-supported decision-making and digital representations of system behaviour (Chenevey and Cooper, 2026). Digital twin approaches further demonstrate the potential of integrating hydraulic models with field observations and operational information to improve adaptive management of water distribution systems (Kim et al., 2026). However, effective implementation requires reliable hydraulic understanding and identification of meaningful system variables.

Hydraulic resilience extends conventional performance evaluation by considering the ability of a system to maintain acceptable functionality under disturbances and changing operating conditions. In water distribution networks, resilience assessment commonly evaluates hydraulic responses under stress scenarios such as increased demand, pipe failures, and other disturbances that may reduce service reliability (Todini, 2000; Di Nardo et al., 2018). Scenario-based hydraulic simulation provides a practical approach for identifying pressure-sensitive locations and hydraulically influential components whose behaviour strongly affects network performance.

For gravity-based water distribution networks, resilience assessment is particularly important because hydraulic performance is strongly influenced by available elevation head and network configuration. A system may satisfy design requirements under normal conditions while still containing localized vulnerabilities that become evident only during extreme demand conditions or component outages. Identifying these vulnerabilities before operational decisions are made can support improved infrastructure management and more targeted monitoring strategies.

Recent developments have extended hydraulic models toward more integrated operational applications by connecting infrastructure models with data-supported decision-making and digital representations of system behaviour (Chenevey and Cooper, 2026). Digital-twin approaches further demonstrate the potential of integrating hydraulic models, monitoring data, and operational information to support adaptive and sustainable water-system management (Kim et al., 2026; Qureshi et al., 2026).

Applications in Jordan and elsewhere demonstrate growing interest in adaptive and data-supported water management strategies (Fasha et al., 2026). However, effective smart water management requires integration between data acquisition, information processing, hydraulic understanding, and operational decisions rather than sensor deployment alone (Ascenção et al., 2023). Therefore, selecting appropriate monitoring locations, measured variables, and interpretation strategies remains essential for converting hydraulic data into actionable operational information (Joseph et al., 2022; Bai et al., 2026).

Despite advances in hydraulic modelling and smart monitoring technologies, a gap remains in systematically linking hydraulic sensitivity assessment with monitoring-system design. Hydraulic models can identify vulnerable locations and stress conditions; however, these outputs are not always translated into targeted monitoring priorities. This study addresses this gap by developing a scenario-based hydraulic resilience assessment and sensitivity-based monitoring framework for a gravity-based water distribution network in Al-Salt, Jordan.

Accordingly, this study investigates the hydraulic resilience of a gravity-based water distribution network through a scenario-based hydraulic analysis approach and develops a system-specific monitoring framework derived from identified hydraulic sensitivities. The study addresses three main research questions: (1) how increasing hydraulic loading affects the resilience of a gravity-based water distribution network by evaluating the impacts of future demand growth, maximum-day conditions, and peak-demand stress on pressure distribution and hydraulic performance; (2) which network components represent the greatest hydraulic vulnerability under pipe failure conditions by assessing the consequences of individual pipe

outages and identifying components whose failure results in significant degradation of network performance; and (3) how hydraulic sensitivity analysis can be translated into monitoring priorities by determining how critical nodes and pipe sections identified through hydraulic simulations can be converted into targeted monitoring locations, measurable hydraulic variables, and operational indicators for improved network management.

To address these questions, an independently developed hydraulic model of a gravity-based water distribution network in Al-Salt, Jordan, was validated against the original WaterGEMS model. The validated model was evaluated under multiple hydraulic loading scenarios and single-pipe outage conditions to quantify network sensitivity and identify critical components. The resulting hydraulic responses were subsequently used to establish a hydraulic sensitivity-based monitoring framework incorporating pressure, flow, velocity, and asset-level indicators.

The scientific contribution of this study is threefold: (1) development and validation of an independent hydraulic model suitable for scenario-based resilience assessment; (2) quantitative evaluation of network vulnerability under demand stress and pipe failure conditions; and (3) translation of hydraulic sensitivity results into a system-specific monitoring strategy for gravity-based water distribution networks.

MATERIALS AND METHODS

The research methodology was developed to assess the hydraulic resilience of a gravity-based water distribution network and translate hydraulic sensitivity results into a system-specific monitoring framework. The methodology consists of five sequential stages: (1) characterization of the study area and hydraulic conditions, (2) development and validation of a hydraulic model, (3) scenario-based assessment of network response under increased hydraulic loading, (4) evaluation of network vulnerability under single-pipe failure conditions, and (5) identification of critical hydraulic locations and variables for monitoring framework development. Unlike conventional hydraulic evaluations that focus only on compliance under design conditions, the proposed approach investigates how network performance changes under hydraulic stress conditions and how these changes can guide targeted monitoring decisions.

Study area and gravity-based water distribution network characteristics

The study was conducted in Naqab Al-Dabur, Al-Salt, Jordan, focusing on the hydraulic resilience assessment of a gravity-based water distribution network. The selected area represents a gravity-fed residential water distribution system designed to utilize available topographic head and reduce dependence on continuous pumping. The site provides an appropriate case study for evaluating hydraulic resilience because elevation differences directly influence pressure distribution, flow behaviour, and network response under changing operating conditions.

The system has an available elevation difference of approximately 53 m between upstream and downstream sections, providing the hydraulic head required for gravity-driven operation. This elevation variation was incorporated into the resilience assessment because it represents both an operational advantage and a potential source of hydraulic sensitivity under increased demand conditions. The Water distribution network of the study area, network boundary, and elevation profile supporting gravity-based operation are presented in Figure 1.

The network serves approximately 5.000 inhabitants distributed across 135 multi-family residential buildings. It consists of a pressurized gravity-fed pipe network connecting the upstream supply source to downstream demand locations. Network topology, pipe characteristics, junction elevations, and hydraulic boundaries were defined from the available design information and implemented in the hydraulic model. The main characteristics of the modeled system, including the number of junctions, pipes, pipe material, and hydraulic parameters, are summarized in Table 1.

The combination of topographic head, network configuration, and distributed demand conditions makes the selected case study suitable for evaluating how gravity-based systems respond to demand stress and component failures. These characteristics provide the basis for subsequent hydraulic model development and scenario-based resilience assessment.

Hydraulic model development and validation

To establish a reliable hydraulic basis for resilience assessment, an independent hydraulic model was developed using the available Bentley

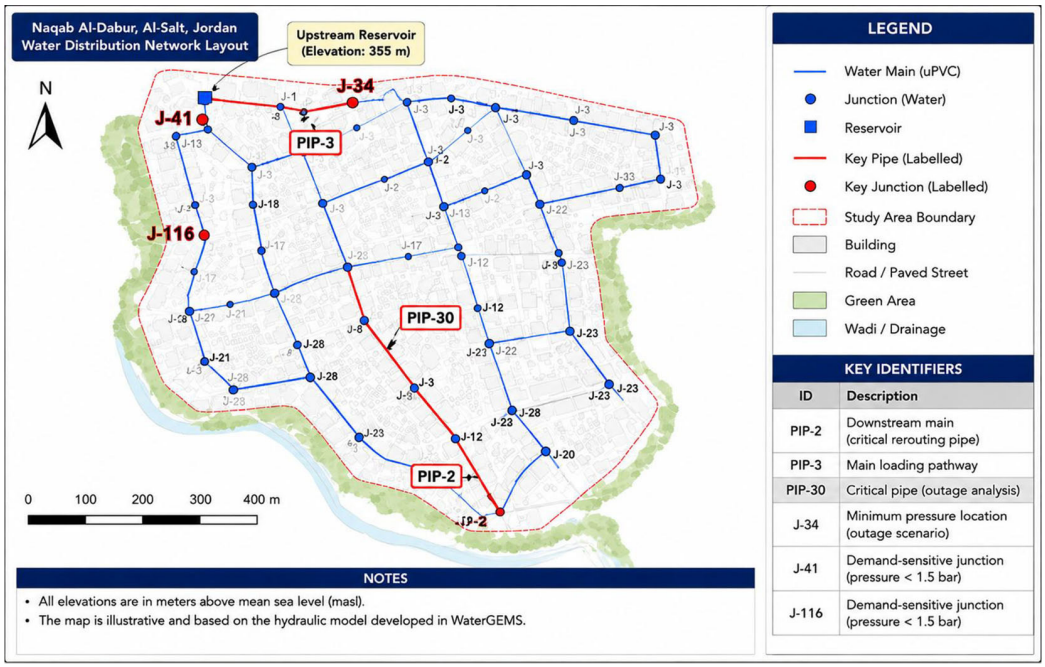

Figure 1. Water distribution network layout of the study area showing key pipe and junction identifiers used in the hydraulic sensitivity analysis

WaterGEMS design information. The development process included extraction of network data, preparation of hydraulic parameters, and implementation of the network configuration, baseline hydraulic simulation, and validation against the original WaterGEMS outputs. The overall workflow of hydraulic model development and validation is presented in Figure 2. The workflow illustrates the use of available WaterGEMS design information as input data for establishing an independently developed and validated hydraulic model used for subsequent scenario-based hydraulic resilience assessment.

The developed water distribution model consisted of 51 junctions and 53 pipes while maintaining consistency with the original network topology, junction elevations, pipe lengths, pipe diameters, hydraulic roughness characteristics, and upstream boundary conditions. The network was represented as a gravity-fed pressurized system supplied by an upstream reservoir with a fixed hydraulic head of 355.00 m. The modeled pipes consisted of uPVC material with diameters ranging from 51.4 to 102 mm, and hydraulic losses were calculated using the Hazen–Williams equation with a roughness coefficient of C

Table 1. Summary of gravity-based water distribution network characteristics

Parameter	Value
Location	Naqab Al-Dabur, Al-Salt, Jordan
Design population	~5,000 inhabitants
Residential buildings	135 multi-family buildings
Network type	Gravity-based pressurized water distribution system
Elevation difference	~53 m
Number of junctions	51
Number of pipes	53
Hydraulic software	Bentley WaterGEMS
Pipe material	uPVC
Pipe diameter range	51.4–102 mm
Reservoir hydraulic head	355.00 m
Hazen–Williams coefficient	C = 130

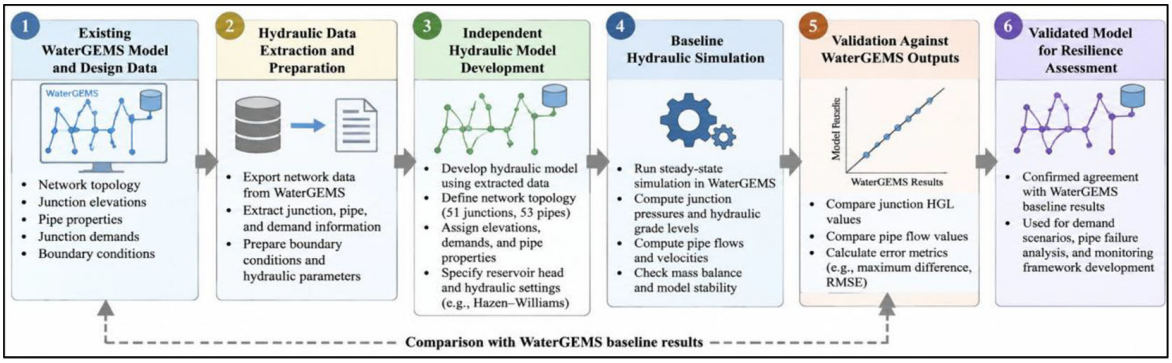

Figure 2. Hydraulic model development and validation workflow

= 130. The main hydraulic model characteristics are summarized in Table 1.

The hydraulic model development was performed by satisfying nodal continuity and pipe energy-loss relationships. Pipe head losses were calculated using the Hazen–Williams formulation:

$$h_f = 10.67 \frac{L\, Q^{1.852}}{C^{1.852} D^{4.87}} \quad (1)$$

where: h_f is pipe headloss (m), L is pipe length (m), Q is discharge (m³/s), C is the Hazen–Williams coefficient, and is the internal pipe diameter (m).

The calculated hydraulic grade levels were subsequently used to determine junction pressure conditions for resilience assessment. The baseline hydraulic loading condition was defined using the spatial demand distribution contained in the exported WaterGEMS model. Although the design population-based demand calculation resulted in approximately 500 m³/day, the sum of individual junction demands in the original model was 501.55 m³/day. Since hydraulic response depends on the spatial allocation of demand throughout the network, the exported junction-demand distribution was retained as the baseline hydraulic condition for all subsequent analyses.

The developed model was validated by comparing its baseline hydraulic solution against the corresponding outputs exported from Bentley WaterGEMS. Validation focused on hydraulic grade level and pipe-flow agreement between the independently developed model and the original design solution. The maximum absolute difference in junction hydraulic grade level was 0.008 m, with an HGL root-mean-square error (RMSE) of 0.004 m. For pipe flow, the maximum absolute difference was 103.5 L/day, with a flow RMSE of 47.3 L/day. These results demonstrate that the developed model closely reproduced the original WaterGEMS hydraulic solution and was therefore considered suitable for comparative hydraulic sensitivity and resilience assessment.

It should be noted that this validation represents numerical development validation against the exported hydraulic model rather than field calibration. Therefore, the developed model is used in this study to evaluate relative hydraulic changes caused by demand variation and pipe availability scenarios rather than to predict measured field conditions.

The hydraulic simulations were performed using a demand-driven analysis (DDA) formulation, consistent with the original Bentley WaterGEMS design model used as the validation reference. Under severe failure scenarios, DDA may calculate negative pressure values when the available hydraulic head becomes insufficient to satisfy the assigned demand. These negative values should not be interpreted as physically sustainable pressure conditions; instead, they indicate locations where the assumed demand cannot be hydraulically supported under the evaluated scenario. Therefore, the DDA results in this study are used as sensitivity indicators to identify critical hydraulic locations and compare relative system degradation rather than to estimate actual delivered demand under pressure-deficient conditions. Future work may incorporate pressure-driven analysis (PDA) or field-calibrated models to evaluate demand delivery and service availability under severe pressure-deficient conditions.

Scenario-based hydraulic resilience assessment

Following validation of the hydraulic model, scenario-based simulations were performed to evaluate the resilience of the gravity-based water

distribution network under changing operating conditions. Rather than evaluating performance only under the baseline design state, the proposed approach examines how hydraulic behaviour evolves when the system is subjected to progressive demand stress conditions. The objective was to quantify changes in service reliability, identify pressure-sensitive locations, and establish a hydraulic basis for subsequent monitoring prioritization.

The resilience assessment was conducted by applying a series of progressive demand-loading scenarios representing present and potential future operating conditions. The baseline condition (S0) represents the current design demand distribution obtained from the validated hydraulic model. Additional scenarios were developed by applying demand multipliers to the validated baseline condition to represent future growth, maximum-day operation, and extreme peak-demand loading conditions. These scenarios include a 20% demand increase (S1), representing moderate future growth; a 50% demand increase (S2), representing maximum-day conditions; and a 100% demand increase (S3), representing an extreme peak-demand condition. The corresponding total daily demands and scenario definitions are summarized in Table 2.

The hydraulic response of each scenario was evaluated based on changes in junction pressure, hydraulic grade level, and pipe-flow behaviour compared with the baseline condition. Particular attention was given to minimum pressure conditions because maintaining adequate pressure throughout the network represents a primary requirement for reliable water delivery. Pressure responses were evaluated against the project-specific minimum service criterion adopted for the network assessment. Locations experiencing significant pressure reduction were considered hydraulically sensitive areas requiring further evaluation and potential monitoring consideration.

To quantitatively evaluate resilience, pressure-based indicators were introduced to describe the degradation of hydraulic service under increasing demand conditions. The Pressure Service Reliability Index (PSRI) was used to quantify the proportion of network junctions maintaining pressure above the minimum service threshold. This indicator provides a direct measure of pressure-service reliability under increasing hydraulic stress.

$$PSRI = \frac{N_{P_i} \geq P_{min}}{N_{total}} \tag{2}$$

where: $N_{P_i} \geq P_{min}$ represents the number of junctions satisfying the minimum pressure requirement and N_{total} is the total number of network junctions.

In addition, the pressure degradation index (PDI) was used to quantify the relative reduction in pressure between the baseline and stressed scenarios. This indicator enables comparison of hydraulic deterioration intensity across different demand conditions.

$$PDI = \frac{P_o - P_s}{P_o} \tag{3}$$

where: P_o represents the baseline pressure condition and P_s represents the pressure under the evaluated scenario.

These indicators allow hydraulic resilience to be assessed not only by identifying whether pressure requirements are satisfied, but also by quantifying the magnitude and spatial distribution of hydraulic degradation. Junctions showing high pressure reduction or reduced reliability under increased demand were classified as hydraulically sensitive locations.

Pipe-flow behaviour was evaluated using the simulated magnitude and redistribution of velocity across the demand-loading and outage scenarios rather than by applying a universal velocity threshold. Hydraulically influential pipe sections were identified from their relative change from baseline conditions, their persistence under increasing system loading, and their response

Table 2. Hydraulic scenarios used for water-distribution resilience assessment

Scenario	Description	Demand multiplier	Total demand (m³/day)
S0	Baseline design condition	1.0	501.55
S1	Future growth condition	1.2	601.86
S2	Maximum-day condition	1.5	752.33
S3	Extreme peak-demand condition	2.0	1003.10

during component-outage scenarios. Accordingly, velocity is interpreted in this study as a comparative hydraulic-response variable, while scenario-specific values are used to characterize network loading and redistribution.

The scenario-based resilience assessment was subsequently used to identify hydraulically sensitive locations and variables requiring monitoring consideration. Therefore, the results from this stage provide the analytical basis for translating hydraulic behaviour into system-specific monitoring priorities.

The overall framework adopted for scenario-based hydraulic resilience assessment is illustrated in Figure 3. The framework links the validated hydraulic model with progressive demand-loading scenarios to evaluate changes in network hydraulic behaviour. By comparing pressure, hydraulic grade level, and flow responses under different operating conditions, the approach identifies hydraulically sensitive locations and provides the basis for subsequent resilience evaluation and monitoring priority selection

Pipe failure vulnerability analysis

In addition to demand-related hydraulic stress, network resilience was evaluated under localized component failure scenarios. Pipe failures can alter flow paths, increase hydraulic losses, redistribute network loading, and reduce service reliability, particularly when failures occur in hydraulically influential sections of the network. Therefore, a pipe failure vulnerability analysis was conducted to identify components whose loss produces significant hydraulic consequences and to evaluate their contribution to overall system resilience.

The analysis was performed using a single-pipe outage approach, where individual pipes were sequentially removed from the validated hydraulic model and the resulting changes in network performance were evaluated. The assessment focused on changes in junction pressure, hydraulic grade level, pipe flow redistribution, and the number of affected junctions compared with the baseline operating condition. This approach enables identification of critical pipe sections whose failure causes disproportionate hydraulic degradation.

Four complementary criteria were considered to evaluate pipe failure vulnerability: pressure degradation, service impact, flow redistribution, and topological importance. These criteria were selected to capture both hydraulic performance deterioration and the structural role of individual pipes within the network. The criteria used for classifying pipe failure vulnerability are summarized in Table 3.

The combined evaluation of these indicators enables identification of pipe components that have a disproportionate influence on network performance. Pipes associated with significant pressure reduction, a larger number of affected junctions, substantial flow redistribution, or important connectivity roles were considered hydraulically vulnerable and were further evaluated for their potential role in monitoring priority selection.

The overall procedure adopted for evaluating hydraulic vulnerability under pipe failure conditions is illustrated in Figure 4. The framework links the validated hydraulic model with sequential single-pipe outage simulations to quantify hydraulic impacts, identify critical network components, and integrate the results into monitoring priority selection.

To improve the structural interpretation of pipe criticality, the analysis considered the topological role of individual pipes within the network. Pipes connecting distinct sections of the network were considered potential hydraulic bottlenecks because their failure may interrupt available flow paths and increase pressure losses in downstream areas. A total of 14 bridge-link pipes were identified through network connectivity analysis and were further evaluated under outage conditions.

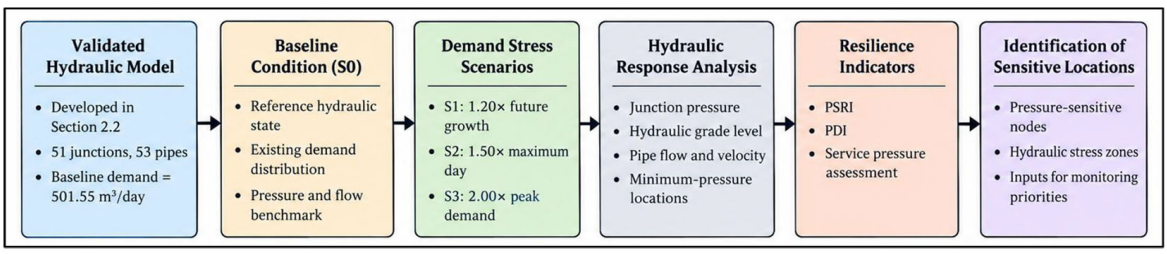

Figure 3. Scenario-based hydraulic resilience assessment framework

Table 3. Criteria used for pipe failure vulnerability assessment

Indicator	Description	Purpose
Minimum pressure reduction	Change in lowest junction pressure after pipe outage	Identifies severe hydraulic degradation
Number of affected junctions	Nodes below service pressure threshold	Measures service impact
Flow redistribution	Changes in remaining pipe flows	Identifies network stress redistribution
Topological role	Bridge-link or connectivity importance	Identifies topologically influential pipes

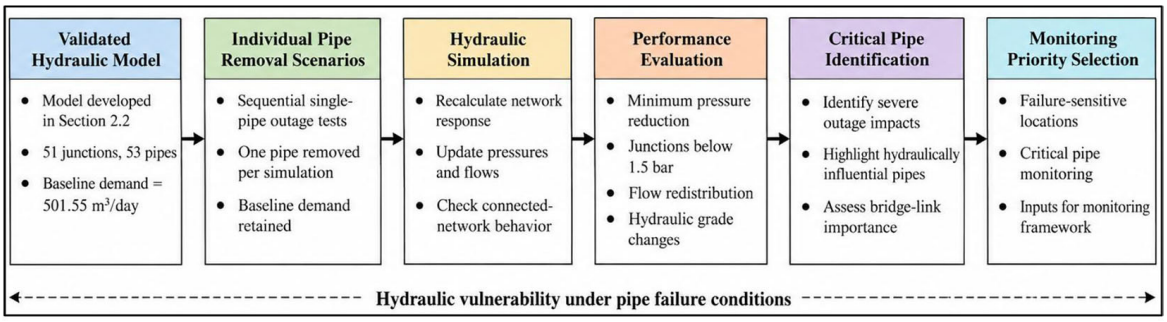

Figure 4. Pipe failure vulnerability assessment workflow

The severity of each pipe outage was evaluated based on three main hydraulic response indicators: (1) reduction in minimum junction pressure, (2) number of junctions experiencing pressure below the minimum service requirement, and (3) changes in flow distribution within the remaining connected pipes. Pipes producing the greatest reduction in hydraulic performance were classified as hydraulically critical components.

Because the analysis was conducted using a DDA formulation, negative calculated pressures represent hydraulic deficiency indicators rather than physically realizable operating pressures. Their purpose is to identify severe loss of hydraulic service potential and compare relative vulnerability among outage scenarios.

To provide a normalized quantitative measure of pressure-service performance under connected-network outage conditions, the pressure service reliability index (PSRI) was also calculated for each screened outage scenario. For an outage condition, PSRI was defined as the proportion of the 51 modeled junctions maintaining pressure at or above the adopted 1.5-bar service-pressure criterion. This enables direct comparison of pressure-service degradation among different pipe-removal scenarios using the same reliability concept applied in the demand-stress assessment. A volumetric water supply ratio (WSR) was not calculated because the Demand-Driven Analysis formulation prescribes nodal demand independently of available pressure and therefore does not estimate actual pressure-dependent delivered demand under severe deficient conditions. Consequently, PSRI is used here as a pressure-service reliability measure, while future PDA-based analysis would be required for physically based volumetric supply assessment.

The pipe failure assessment provides a complementary resilience perspective to the demand-stress scenarios. While demand scenarios evaluate the ability of the network to maintain performance under increased hydraulic loading, pipe outage scenarios identify components whose failure creates localized vulnerability. The results of this analysis are subsequently used to determine critical monitoring locations and variables within the hydraulic sensitivity-based monitoring framework.

The pipe outage screening was performed using the hydraulic criteria described in this section and was not based on the WaterGEMS Criticality Analysis module.

Hydraulic sensitivity-based monitoring framework

The monitoring framework was developed using the hydraulic sensitivity results obtained from the demand-loading and pipe-failure vulnerability analyses. Rather than selecting monitoring locations based on general network characteristics, the proposed approach identifies monitoring priorities according to locations and components that demonstrate significant hydraulic response under scenario-based operating conditions. The framework therefore establishes a direct

connection between hydraulic resilience assessment and targeted monitoring design.

The proposed hydraulic sensitivity-based monitoring framework integrates the outcomes of demand-stress analysis and pipe-failure vulnerability assessment to identify priority monitoring locations and associated hydraulic variables. As illustrated in Figure 5, the framework begins with the validated hydraulic model, from which hydraulic responses under different loading conditions and failure scenarios are evaluated. The identified pressure-sensitive nodes, critical pipe components, and failure-sensitive locations are then translated into monitoring priorities. The selected variables, including pressure, flow, velocity behaviour, and asset status, are subsequently evaluated against expected hydraulic conditions to support sensitivity-based anomaly interpretation and operational decision-making.

The framework does not represent a fully deployed monitoring system; rather, it provides a hydraulic basis for selecting where monitoring should be implemented and which variables should be prioritized. By linking simulated hydraulic responses with potential operational observations, the framework supports targeted data collection and improves interpretation of abnormal network behaviour.

Three criteria were used to identify priority monitoring locations. First, demand-sensitive junctions were identified based on pressure-margin reduction under increasing hydraulic loading scenarios, including future-growth, maximum-day, and peak-demand-equivalent conditions. Second, outage-sensitive locations were identified from the pipe failure vulnerability analysis based on hydraulic degradation caused by individual pipe failures. Third, topologically critical components were identified based on bridge-link characteristics, where pipe removal resulted in network disconnection or major flow redistribution.

Based on these criteria, the monitoring framework was organized around four categories of hydraulic and operational indicators: pressure, flow, velocity-related behaviour, and asset-status information. Pressure monitoring was assigned to hydraulically sensitive junctions where pressure reduction indicated potential service degradation. Flow monitoring was associated with source-transfer pipes and hydraulically influential pipe sections where significant redistribution occurred under stressed or abnormal conditions.

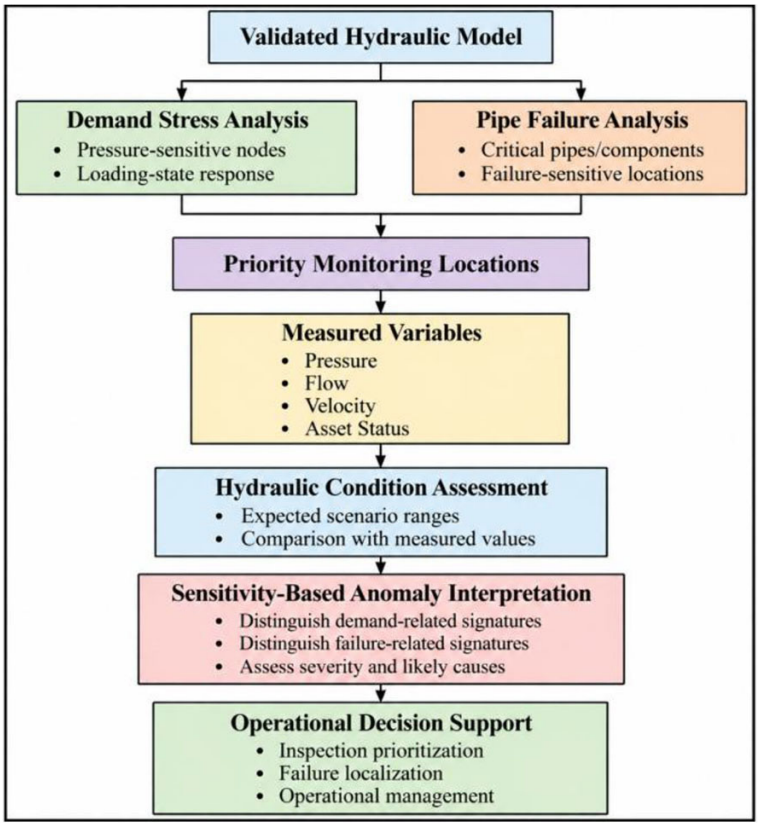

Figure 5. Hydraulic sensitivity-based monitoring framework

Velocity-related indicators were considered for identifying increased hydraulic loading and potential stress concentration in critical conveyance paths. Asset-status information was considered particularly relevant for critical pipe sections and bridge-link components whose availability directly affects network connectivity.

Rather than defining fixed operational alarm thresholds solely from the steady-state stress scenarios, the proposed framework uses two complementary model-based references: (1) a temporal hydraulic reference envelope derived from the 24-hour extended-period simulation (EPS) to represent expected variation under the prescribed time-varying demand pattern, and (2) disturbance signatures derived from the single-pipe outage simulations. For demand-sensitive junctions and hydraulically influential pipe sections, pressure and velocity observations are therefore interpreted relative to the hydraulic state expected for the corresponding demand condition rather than against a single fixed warning value. The project-specific minimum pressure criterion of 1.5 bar is retained as a service-pressure screening criterion and is not interpreted as a data-derived anomaly threshold.

Potential abnormal conditions are identified when hydraulic observations depart from the corresponding model-based temporal reference or when combinations of hydraulic variables exhibit a response inconsistent with generalized demand variation. Generalized demand stress is characterized by coordinated pressure reduction at J-41 and J-116 together with increased conveyance loading in PIP-3. In contrast, a localized pipe disturbance is characterized by a disproportionate pressure reduction at an outage-sensitive location such as J-34, accompanied by flow redistribution in PIP-2 and, where available, a change in the flow or asset status of PIP-30. Because the temporal demand pattern used in this study is a prescribed design-sensitivity profile rather than a field-calibrated consumption record, the resulting hydraulic ranges are interpreted as model-based screening and commissioning references rather than field-validated operational alarm limits. Field monitoring data would therefore be required to calibrate final operational alarm thresholds.

To distinguish between general demand increase and localized component failure, the proposed framework considers combined hydraulic responses rather than relying on a single measurement. Increased system demand is characterized by a general increase in source flow accompanied by pressure reduction at demand-sensitive nodes. In contrast, localized pipe failures are associated with abnormal pressure reduction at affected locations, flow redistribution in neighbouring pipes, and changes in hydraulic behaviour around the failed component.

The proposed framework consists of four functional stages: hydraulic data acquisition, where selected pressure, flow, velocity, and asset-status variables are obtained from priority locations; hydraulic condition assessment, where measured values are compared with expected scenario-based hydraulic ranges; sensitivity-based anomaly interpretation, where deviations are evaluated against known hydraulic signatures; and decision support, where the identified hydraulic conditions support inspection prioritization, failure localization, and operational management.

The monitoring framework developed in this study does not represent a fully deployed monitoring system but provides a system-specific hydraulic basis for selecting measurement locations, monitored variables, and abnormal-condition indicators. By linking simulated hydraulic sensitivity with monitoring priorities, the framework supports targeted data collection and improved operational awareness for gravity-based water distribution networks.

To evaluate whether the sensitivity locations identified under steady-state scenarios remained representative during normal operational variation, an extended-period simulation (EPS) was performed over a 24-hour period. The EPS was not treated as a separate vulnerability-assessment method; rather, it was used as a temporal consistency assessment to examine the evolution of hydraulic variables at locations previously identified through the scenario-based resilience analysis. The validated network configuration, pipe characteristics, reservoir boundary condition, and spatial distribution of baseline junction demands were retained during the temporal simulation.

Time-varying hydraulic loading was represented using a normalized 24-hour design-sensitivity demand pattern applied uniformly to the baseline junction-demand distribution. The hourly demand multipliers from 00:00 to 23:00 were 0.40, 0.35, 0.30, 0.30, 0.40, 0.70, 1.20, 1.80, 1.60, 1.20, 0.90, 0.80, 0.80, 0.90, 0.90, 1.00, 1.20, 1.60, 2.00, 1.80, 1.40, 1.10, 0.80, and 0.55, respectively. The pattern has a 24-hour mean multiplier of 1.00, thereby preserving the adopted average daily demand, while the maximum multiplier of 2.00 occurs at 18:00

and corresponds to the peak-demand-equivalent loading condition evaluated in scenario S3. Because a field-calibrated hourly demand profile was not available, the pattern was adopted as a reproducible design-sensitivity input rather than as a representation of measured hourly consumption. The normalized temporal demand pattern is presented in Figure 13. The resulting EPS was used to evaluate whether the pressure-sensitive junctions and hydraulically influential pipe sections identified from the steady-state scenarios remained informative under time-varying demand conditions.

RESULTS

Water-distribution model validation and scenario-based hydraulic response

The hydraulic response of the gravity-based water-distribution network was evaluated under the baseline condition and three progressively increased demand conditions, followed by a single-pipe outage sensitivity analysis. Before conducting the scenario assessment, the independently developed hydraulic model was compared with the exported Bentley WaterGEMS baseline outputs. The developed model closely reproduced the WaterGEMS solution, with a maximum absolute hydraulic-grade difference of 0.008 m and an HGL RMSE of 0.004 m. Pipe-flow agreement was similarly close, with a maximum absolute difference of 103.5 L/day and an RMSE of 47.3 L/day. These results confirmed that the developed model was suitable for comparative scenario-based hydraulic analysis.

Under the baseline loading condition (S0) of 501.55 m³/day, simulated junction pressures ranged from 2.44 to 4.17 bar, with a network mean pressure of 3.35 bar. The baseline PSRI value was 1.00, indicating that all 51 junctions satisfied the project-specific minimum pressure criterion of 1.5 bar. The minimum pressure occurred at J-134, whereas the maximum pressure occurred at J-127. Pipe velocities ranged from approximately 0.008 to 0.71 m/s, with a mean value of 0.34 m/s. Seventeen of the 53 modeled pipes exhibited velocities below 0.20 m/s under baseline conditions. PIP-3 exhibited the highest baseline velocity at 0.71 m/s and subsequently remained the most highly loaded pipe as system demand increased.

Increasing network demand resulted in progressive pressure reduction and increased pipe velocity. Under the future-growth scenario (S1), corresponding to a total demand of 601.86 m³/day, the minimum pressure decreased to 2.34 bar and shifted to J-41, while the mean pressure decreased to 3.23 bar. The maximum pipe velocity increased to 0.85 m/s and remained associated with PIP-3. No junction fell below the 1.5-bar pressure criterion, and the PSRI remained equal to 1.0. The number of pipe sections with velocities below 0.20 m/s decreased from 17 under baseline conditions to 11 under S1.

Under the maximum-day scenario (S2), with a total demand of 752.33 m³/day, the minimum network pressure decreased further to 2.05 bar at J-41, while the mean pressure declined to 3.03 bar. All junctions remained above the 1.5-bar pressure criterion. The maximum pipe velocity increased to 1.07 m/s in PIP-3, confirming the progressive increase in hydraulic loading along the principal conveyance pathway. The PSRI remained equal to 1.0 under this loading condition.

The largest hydraulic changes occurred under the peak-demand-equivalent scenario (S3), corresponding to a total modeled demand of 1003.1 m³/day. The minimum pressure decreased to 1.46 bar at J-41, while the mean network pressure decreased to 2.6 bar. Two junctions fell below the 1.5-bar screening criterion: J-41, with a pressure of 1.46 bar, and J-116, with a pressure of 1.49 bar. J-117 remained slightly above the threshold with a simulated pressure of approximately 1.54 bar. Relative to their baseline conditions, pressure at J-41 decreased from 2.50 to 1.46 bar, while pressure at J-116 decreased from 2.54 to 1.49 bar. The PSRI decreased to 0.96 because 49 of the 51 junctions maintained the minimum pressure requirement.

Pipe velocities showed a corresponding increase with hydraulic loading. The maximum velocity occurred consistently in PIP-3 and increased from 0.71 m/s under baseline conditions to 0.85, 1.07, and 1.42 m/s under the 1.20×, 1.50×, and 2.00× scenarios, respectively. This progressive increase identifies PIP-3 as the principal hydraulic loading pathway and provides a system-specific basis for interpreting changes in conveyance loading without relying on a fixed velocity threshold. At the same time, the number of pipe sections with velocities below 0.20 m/s decreased from 17 under baseline loading to nine under the peak-demand-equivalent condition.

The scenario-based hydraulic responses of the water-distribution network are summarized quantitatively in Table 4.

The spatial response of junction pressure under increasing hydraulic loading is illustrated in Figure 6, showing the progressive reduction in pressure and the emergence of J-41 and J-116 as the most pressure-sensitive locations under S3. The corresponding redistribution of pipe velocities is presented in Figure 7, showing increased hydraulic loading along the principal conveyance pathway and consistently high velocity in PIP-3.

Pressure-based resilience indicators

Pressure-based resilience indicators were derived to complement the direct hydraulic response analysis by quantifying changes in pressure-service reliability and pressure degradation under increasing hydraulic loading. The Pressure Service Reliability Index (PSRI) represents the proportion of junctions maintaining the project-specific minimum pressure criterion of 1.5 bar, while the Pressure Degradation Index (PDI) quantifies the relative reduction in pressure compared with the baseline condition. The calculated PSRI and PDI values for the evaluated demand scenarios are summarized in Table 5.

Under baseline conditions (S0), all 51 junctions satisfied the minimum pressure requirement, resulting in a PSRI value of 1.00. The future-growth (S1) and maximum-day (S2) scenarios also maintained full pressure reliability, with PSRI values remaining equal to 1.00.

Under the peak-demand-equivalent condition (S3), two junctions fell below the 1.5-bar criterion (J-41 and J-116), reducing the PSRI value to 0.96. The corresponding PDI values showed a progressive increase in pressure degradation with increasing hydraulic loading, with the largest degradation occurring under the S3 condition.

The peak-demand-equivalent condition produced the largest pressure reductions at individual junctions. The pressure response of the most affected locations was further evaluated using the pressure degradation index (PDI) to quantify the relative reduction from the baseline condition. As shown in Table 6, J-41 and J-116 experienced the greatest pressure reductions under S3, with reductions of 1.03 and 1.05 bar, respectively. J-117 remained close to the minimum pressure threshold but did not fall below the project-specific criterion.

The calculated PDI values demonstrate the relative pressure deterioration at the most affected junctions under peak-demand-equivalent loading. These results provide a quantitative basis for identifying pressure-sensitive locations, with J-41 and J-116 representing priority candidates for pressure monitoring within the hydraulic sensitivity-based monitoring framework.

Single-pipe outage sensitivity

The single-pipe outage analysis produced larger hydraulic changes than those observed under demand-increase scenarios. Fourteen pipe sections were identified as topological bridge links, meaning that removal of any of these links disconnects part of the network from the modeled supply path. These pipes were classified as topologically critical connectivity components.

Among the outage cases where the remaining network retained hydraulic connectivity, removal of PIP-30 produced the most severe hydraulic response. The minimum calculated residual pressure decreased to −1.07 bar at J-34, indicating severe

Table 4. Scenario-based hydraulic response of the water-distribution network

Parameter	Baseline S0	Future +20% S1	Maximum day S2	Peak-equivalent S3
Total demand (m^3/day)	501.55	601.86	752.33	1003.10
Minimum pressure (bar)	2.44	2.34	2.05	1.46
Minimum-pressure node	J-134	J-41	J-41	J-41
Maximum pressure (bar)	4.17	4.06	3.87	3.64
Mean pressure (bar)	3.35	3.23	3.03	2.6
Minimum velocity (m/s)	0.008	0.01	0.013	0.017
Maximum velocity (m/s)	0.71	0.85	1.07	1.42
Maximum-velocity pipe	PIP-3	PIP-3	PIP-3	PIP-3
Mean velocity (m/s)	0.34	0.40	0.50	0.67
Junctions < 1.5 bar	0	0	0	2
Pipes < 0.20 m/s	17	11	11	9

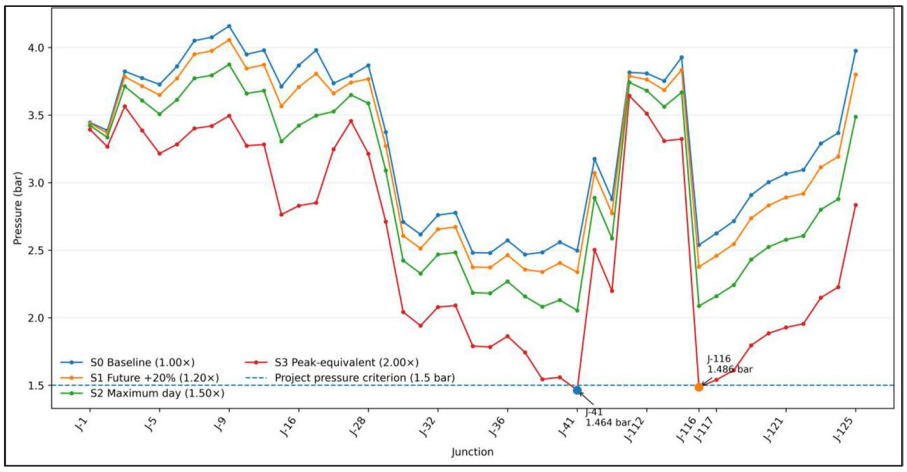

Figure 6. Spatial distribution of junction pressure response under baseline and increased demand-loading scenarios (S0–S3). The dashed line represents the minimum service-pressure criterion (1.5 bar)

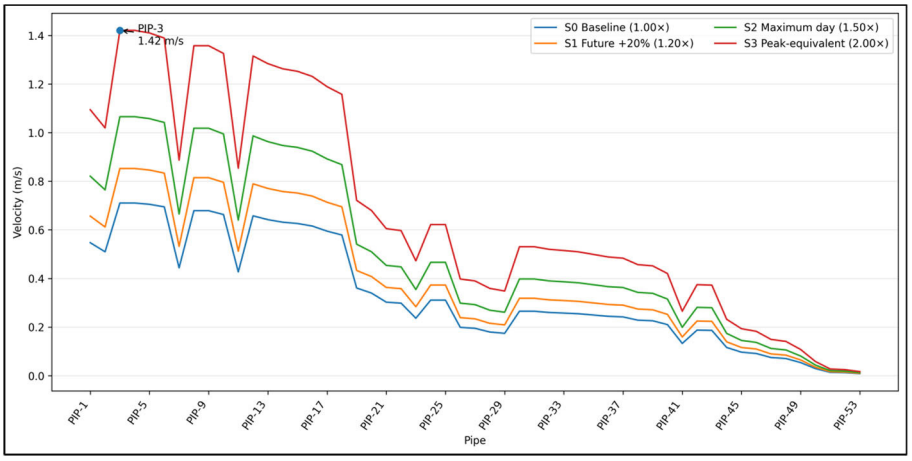

Figure 7. Spatial distribution of pipe velocity response under baseline and increased demand-loading scenarios (S0–S3), showing progressive velocity redistribution and increased hydraulic loading along the principal conveyance pathway

Table 5. Pressure-based resilience indicators under demand-loading scenarios

Scenario	Demand multiplier	Junctions meeting ≥1.5 bar	Junctions below 1.5 bar	PSRI	Mean pressure (bar)	PDI
S0 Baseline	1.00	51	0	1.00	3.35	0.00
S1 Future growth	1.20	51	0	1.00	3.23	0.03
S2 Maximum day	1.50	51	0	1.00	3.03	0.10
S3 Peak-demand-equivalent	2.00	49	2	0.96	2.6	0.22

hydraulic deficiency under the assumed DDA outage condition, while the network mean pressure decreased to 1.83 bar. Twenty-one junctions fell below the project-specific 1.5-bar criterion, and hydraulic redistribution increased the maximum pipe velocity to 1.55 m/s in PIP-2. These results identify PIP-30 as the most hydraulically influential connected-network component among the evaluated outage cases.

The severity ranking demonstrated that vulnerability was not limited to a single component. Removal of PIP-36, PIP-38, PIP-43, and PIP-1 produced progressively lower hydraulic impacts, identifying a group of hydraulically sensitive pipe

Table 6. Pressure degradation at critical junctions under peak-demand-equivalent loading

Junction	Baseline pressure (bar)	S3 pressure (bar)	Pressure reduction (bar)	PDI
J-41	2.50	1.46	1.03	0.41
J-116	2.54	1.49	1.05	0.42
J-117	—	1.54	—	—

sections. The resulting hydraulic responses provide a basis for prioritizing critical pipe-related monitoring variables and locations.

Extension of the PSRI to the connected-network outage scenarios provided a normalized measure of pressure-service degradation. Removal of PIP-30 produced the lowest outage PSRI of 0.59, indicating that only 30 of the 51 modeled junctions remained at or above the 1.5-bar service-pressure criterion. The corresponding PSRI values were 0.69 for PIP-36, 0.71 for PIP-38, 0.82 for PIP-43, and 0.92 for PIP-1. These values confirm the same severity ordering indicated by the minimum-pressure and affected-junction results and provide a quantitative basis for comparing the service consequences of individual connected-network pipe outages.

The comparative effect of individual screened non-bridge pipe outages on minimum residual pressure is illustrated in Figure 8. The principal hydraulic indicators for the five most severe connected-network outage scenarios are summarized in Table 7.

The severity of each outage scenario was evaluated based on changes in minimum residual pressure, the number of junctions below the 1.5-bar service threshold, and flow redistribution effects within the remaining connected pipes. The results identify critical pipe components whose failure produces disproportionate changes in network hydraulic performance and contribute to the hydraulic sensitivity-based monitoring framework.

System-specific monitoring priorities derived from hydraulic sensitivity

Hydraulic sensitivity results were used to identify priority monitoring locations and indicators. Monitoring priorities were assigned according to three hydraulic criteria: loss of pressure margin under increased demand, deviation between intact and abnormal hydraulic states, and topological importance to network connectivity. This approach links simulated hydraulic sensitivity results with the selection of monitoring locations, variables, and model-based reference conditions and disturbance signatures.

The increased-demand simulations identified J-41 and J-116 as the principal pressure-sensitive junctions. At J-41, simulated pressure decreased from 2.50 bar under the baseline condition to 2.34 bar under future-growth loading, 2.05 bar under maximum-day loading, and 1.46 bar under peak-demand-equivalent loading. J-116 exhibited a similar response, decreasing from 2.54 bar under the baseline condition to 2.38, 2.09, and 1.49 bar under the future-growth, maximum-day, and peak-demand-equivalent conditions, respectively. Both locations fell below the project-specific 1.5-bar service-pressure criterion under the S3 condition and were selected as priority pressure-monitoring nodes. The reduction in PSRI under S3 supports the identification of J-41 and J-116 as priority pressure-monitoring locations, while their PDI values indicate substantial local pressure sensitivity.

J-34 was selected as an additional pressure-monitoring location because of its sensitivity to localized pipe failure. Under all intact demand scenarios, its simulated pressure remained between approximately 2.48 and 1.79 bar. In contrast, removal of PIP-30 caused the minimum calculated pressure to decrease to −1.07 bar at J-34. The difference between intact and outage responses identifies J-34 as a pressure-sensitive location under localized failure conditions.

At the pipe level, PIP-3 was selected as the principal conveyance-path monitoring point and loading-state monitoring location. Its simulated velocity increased systematically from 0.71 m/s at baseline to 0.85 m/s under future growth, 1.07 m/s under maximum-day loading, and 1.42 m/s under peak-equivalent loading. PIP-3 is also a topological bridge link connecting reservoir R-5 with J-134; consequently, its hydraulic condition reflects both overall network loading and source-path availability.

PIP-2 was selected as a hydraulic-redistribution indicator. Its intact-network velocity increased from approximately 0.51 m/s at baseline to 1.02 m/s under the S3 condition. During the

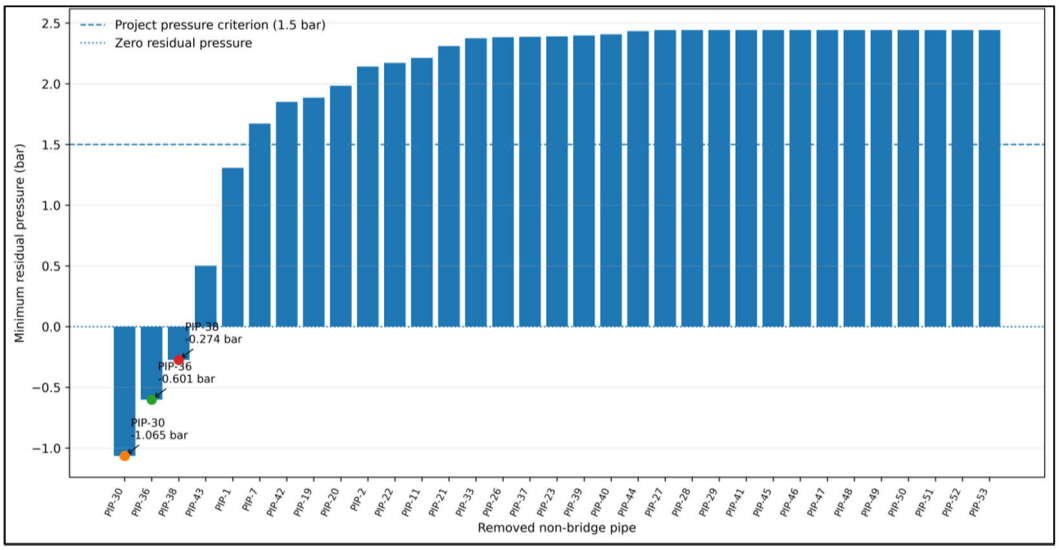

Figure 8. Single-pipe outage sensitivity based on minimum residual pressure response for screened non-bridge pipes

Table 7. Most hydraulically severe connected-network single-pipe outage scenarios

Removed pipe	Minimum pressure (bar)	Critical node	Nodes <1.5 bar	Outage PSRI	Nodes <0 bar	Maximum velocity (m/s)	Critical velocity pipe
PIP-30	−1.07	J-34	21	0.59	15	1.55	PIP-2
PIP-36	−0.60	J-35	16	0.69	8	1.47	PIP-2
PIP-38	−0.27	J-38	15	0.71	5	1.41	PIP-2
PIP-43	0.50	J-38	9	0.82	0	1.24	PIP-2
PIP-1	1.31	J-39	4	0.92	0	1.06	PIP-2

PIP-30 outage, the maximum rerouted velocity increased to approximately 1.55 m/s in PIP-2. The difference between the intact and outage responses provides a hydraulic signature for distinguishing generalized high-demand conditions from localized network disruption.

PIP-30 was assigned the highest modeled localized outage sensitivity among the evaluated connected-network pipe scenarios. Under baseline operation, its velocity was approximately 0.27 m/s; this increased to approximately 0.53 m/s under the 2.00× loading condition. Its removal produced the most severe modeled connected-network outage, with 21 junctions below 1.5 bar, 15 junctions with calculated pressure below zero, and a maximum rerouted velocity of 1.55 m/s in PIP-2. PIP-30 was therefore assigned a monitoring priority based on flow information together with valve or asset-status information, with J-34 and PIP-2 providing hydraulic confirmation of possible outage conditions.

The network-topology analysis additionally identified 14 bridge links: PIP-3, PIP-4, PIP-5, PIP-6, PIP-8, PIP-9, PIP-10, PIP-12, PIP-13, PIP-14, PIP-15, PIP-16, PIP-17, and PIP-18. Removal of these links disconnects portions of the modeled network rather than simply reducing residual pressure. They were therefore classified as connectivity monitoring priorities, with emphasis on valve status, asset condition, flow continuity, and, where practicable, upstream–downstream pressure differential. The selected monitoring locations, hydraulic roles, proposed measurements, model-based reference conditions, disturbance signatures, and operational interpretations are summarized in Table 8.

The integration of scenario-derived hydraulic sensitivities with the proposed monitoring architecture is summarized in Figure 9. The framework links hydraulic-model outputs with monitoring locations, measured variables, and scenario-based interpretation rules. Demand-sensitive nodes, outage-sensitive locations, and structurally critical links identified from the hydraulic analysis are translated into pressure, flow, velocity, asset-status, and continuity monitoring

priorities. Figure 9 summarizes the relationship between hydraulic sensitivity assessment and the resulting system-specific monitoring framework.

Temporal hydraulic response under time-varying demand conditions

A 24-hour hydraulic simulation was performed using the validated water distribution model to evaluate whether the hydraulically sensitive locations identified through steady-state scenario analysis remained representative under time-varying operation. The temporal analysis applied hourly demand variations to evaluate changes in pressure, hydraulic grade response, and flow behaviour throughout the daily operating cycle. The objective was to complement the steady-state resilience assessment by examining the persistence of hydraulic sensitivity under time-varying demand conditions.

The temporal simulation evaluated the evolution of key hydraulic variables, including junction pressure distribution, hydraulic grade response, and pipe-flow behaviour throughout the daily demand cycle. The temporal response provided a dynamic hydraulic profile that complements the previously evaluated steady-state scenarios by showing how network conditions vary between lower-demand and peak-demand periods. The temporal hydraulic response of the network, including pressure variation and changes along the main conveyance pathway, is presented in Figures 10 and 11.

The temporal results showed that the locations identified through steady-state sensitivity analysis also exhibited high pressure sensitivity during daily demand variation. Junction J-41 showed a reduction in pressure from approximately 2.85 bar during the lower-demand period to 1.46 bar during the maximum daily loading condition, while J-116 decreased from approximately 2.9 bar to 1.49 bar. These responses correspond with the S3 peak-demand-equivalent results, where J-41 and J-116 were the only junctions falling below the project-specific 1.5-bar pressure criterion.

The temporal pressure response at hydraulically sensitive junctions is further illustrated in Figure 12. The figure shows the variation of pressure at J-41 and J-116 throughout the daily operating cycle and highlights pressure-margin reduction during periods of increased hydraulic loading.

The temporal analysis also evaluated pipe-level hydraulic response. Variations in hydraulic

Table 8. System-specific monitoring plan

Location	Hydraulic role	Proposed measurement	Model-based reference / screening indicator	Operational interpretation
J-41	Primary demand-stress sentinel	Pressure	Compare with the time-dependent EPS pressure reference; 1.5 bar retained as the service-pressure screening criterion	Demand-related pressure stress when reduction is consistent with increased system loading; investigate disproportionate or time-inconsistent pressure loss
J-116	Secondary demand-stress sentinel	Pressure	Compare with the time-dependent EPS pressure reference; 1.5 bar retained as the service-pressure screening criterion	Confirms generalized demand-related pressure stress when response is consistent with J-41 and system loading
J-34	Local outage sentinel	Pressure	Pressure departure from the intact modeled response, interpreted jointly with PIP-30 status/flow and PIP-2 redistribution	Localized disturbance indicator when pressure loss is disproportionate to the prevailing demand state
PIP-3	conveyance-loading indicator	Flow and inferred velocity	Interpret relative to the time-dependent EPS envelope; ≈1.07 m/s corresponds to the S2 maximum-day state and ≈1.42 m/s to the S3 peak-equivalent state	System-loading indicator rather than a stand-alone alarm threshold
PIP-2	Hydraulic rerouting indicator	Flow and inferred velocity	Deviation from the intact temporal hydraulic response; approximately 1.55 m/s combined with localized pressure loss represents the modeled PIP-30 outage signature	Differentiates local rerouting from ordinary demand increase
PIP-30	Critical local pipe	Flow + valve/status	Unexpected flow loss relative to current source loading	Candidate failure when combined with J-34 pressure loss and PIP-2 acceleration
14 bridge links	connectivity-critical points	Valve/asset status; selective flow/ pressure differential	Unplanned closure, loss of flow continuity, or downstream pressure loss	Immediate service-interruption risk

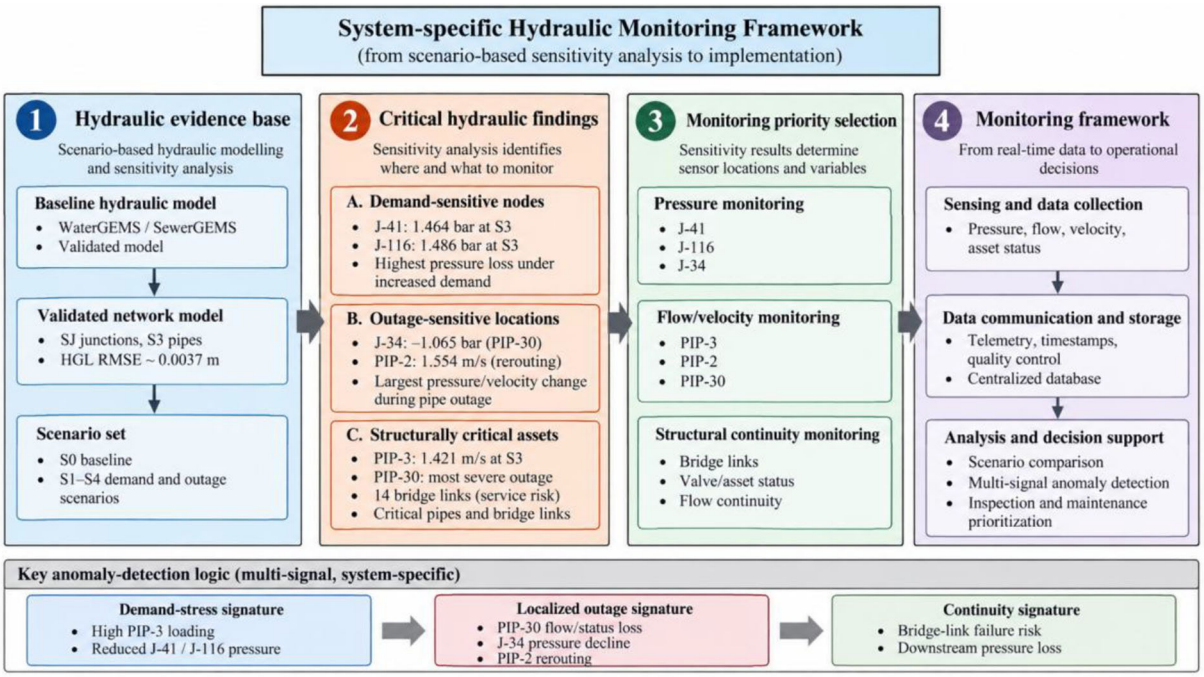

Figure 9. System-specific hydraulic monitoring framework derived from scenario-based sensitivity analysis

loading influenced flow distribution along the principal conveyance pathway, where PIP-3 was previously identified as the most highly loaded pipe under increased-demand conditions. The temporal response provided additional information regarding expected changes in hydraulic loading and supported the evaluation of flow and velocity-related monitoring indicators for hydraulically influential pipe sections.

The temporal analysis confirmed that the selected monitoring locations identified from steady-state sensitivity analysis remained responsive under time-varying hydraulic conditions. J-41 and J-116 showed consistent pressure sensitivity during daily demand variation, while PIP-3 and PIP-2 provided additional information regarding changing loading and hydraulic redistribution behaviour

To relate the observed temporal hydraulic responses to the imposed loading conditions, Figure 13 presents the normalized 24-hour design-sensitivity demand pattern applied in the EPS. The demand multiplier ranged from 0.30 during the lowest-demand periods to 2.00 at 18:00, while maintaining a 24-hour mean of 1.00. This prescribed loading pattern provides the temporal context for interpreting the pressure and velocity responses shown in Figures 10–12 and demonstrates that the maximum temporal loading corresponds to the S3 peak-demand-equivalent condition.

The 24-hour simulation also provides model-based temporal reference ranges for the proposed monitoring variables. Pressure at J-41 varied from approximately 2.85 to 1.46 bar, while pressure at J-116 varied from approximately 2.90 to 1.49 bar over the prescribed daily loading cycle. Correspondingly, velocity in PIP-3 varied from approximately 0.21 to 1.42 m/s, while PIP-2 varied from approximately 0.15 to 1.02 m/s under intact-network conditions. These ranges demonstrate that substantial hydraulic variation can occur solely as a consequence of changing demand. Consequently, values near the limits of these ranges should not, by themselves, be interpreted as evidence of failure. Instead, anomaly screening should consider the expected hydraulic condition for the corresponding demand period together with corroborating pressure, flow, and asset-status indicators.

DISCUSSION

Scenario-based hydraulic resilience under variable demand

Gravity-based water distribution systems benefit from the use of available elevation head, which can reduce dependence on pumping infrastructure and associated operational energy requirements. However, satisfactory hydraulic

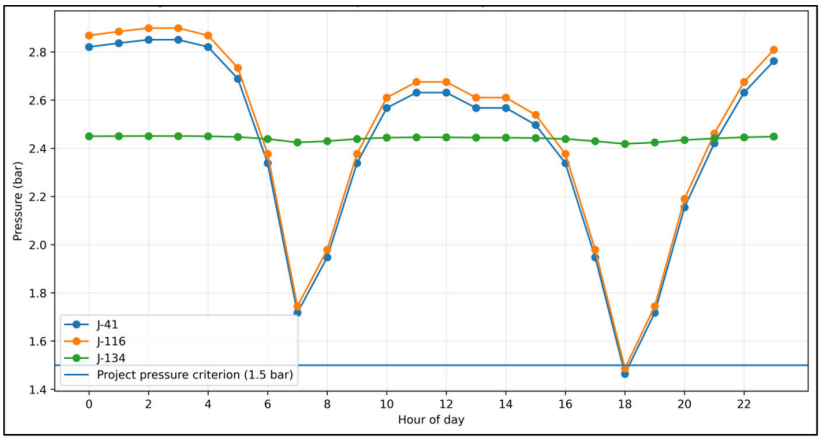

Figure 10. Temporal pressure variation at selected sensitive junctions under 24-hour demand variation

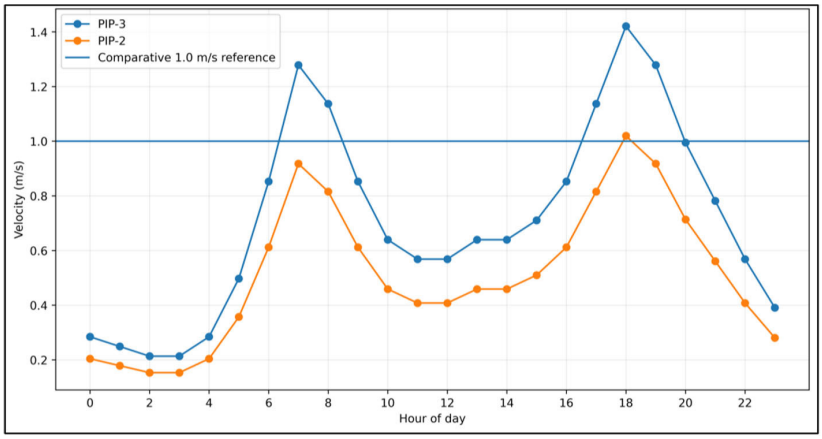

Figure 11. Temporal velocity variation in hydraulically influential pipes under 24-hour demand variation

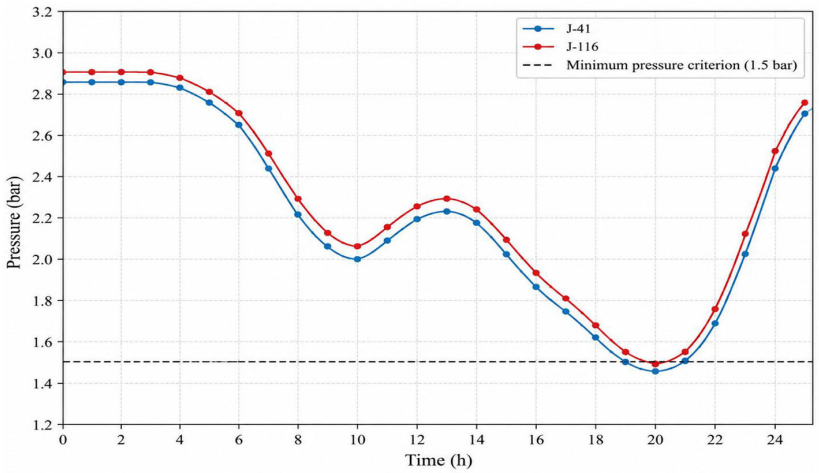

Figure 12. Temporal pressure response at hydraulically sensitive junctions under 24-hour demand variation

performance under a single design condition does not necessarily indicate resilience under changing operating conditions. Resilience assessment requires evaluation of the ability of water distribution systems to maintain acceptable hydraulic performance when exposed to increased demands, component disturbances, or other changes in operational conditions rather than relying only on conventional design criteria (Todini, 2000; Jayaram and Srinivasan,

2008). In this study, the baseline scenario demonstrated that the available hydraulic head was sufficient to maintain acceptable pressure conditions throughout the network; however, the scenario-based assessment showed that hydraulic sensitivity increased progressively as demand loading increased.

The reduction in pressure margin under increasing demand scenarios reflects the relationship between hydraulic loading and resilience in gravity-based networks. As demand increases, higher flow requirements increase energy losses along the conveyance system and reduce the available pressure surplus at hydraulically disadvantaged locations. This behaviour is particularly important in gravity-fed systems because performance depends strongly on elevation distribution, network configuration, and the spatial relationship between available supply head and demand locations. Previous studies have highlighted that hydraulic resilience is influenced not only by total system capacity but also by the distribution of pressure surplus and the ability of individual network locations to maintain acceptable service levels under stressed conditions (Todini, 2000; Prasad and Park, 2004).

The scenario-based hydraulic assessment provides additional insight beyond conventional design-condition evaluation by showing how system performance changes as operating conditions move away from the baseline state. In this study, progressive demand scenarios demonstrated that hydraulic degradation was not uniformly distributed throughout the network. Instead, pressure reduction was concentrated at specific junctions where hydraulic margins were limited. This finding supports previous research indicating that network-level resilience indicators should be complemented by local hydraulic performance evaluation because pressure limitations may occur at specific nodes even when overall system performance remains acceptable (Walski et al., 2003).

The introduction of the PSRI and PDI provided an additional quantitative interpretation of the scenario results. Traditional resilience indicators, such as the resilience index proposed by Todini (2000), quantify available hydraulic surplus and the intrinsic capacity of a water distribution network to maintain performance under stressed conditions. Subsequent studies have further developed resilience-based assessment approaches by linking hydraulic performance indicators with network reliability and operational requirements (Suribabu, 2017). In this study, PSRI and PDI complement these established concepts by focusing specifically on pressure-service performance and localized pressure degradation under variable demand conditions. This enables identification of not only whether the network satisfies pressure requirements but also where and to what extent hydraulic performance deteriorates.

The identification of J-41 and J-116 as pressure-sensitive locations demonstrates that resilience limitations in gravity-based networks may emerge at specific downstream or hydraulically constrained areas due to the combined influence of topology, elevation differences, and spatial demand distribution. Similar observations have been reported in water distribution resilience studies, where local pressure deficits and sensitivity to demand variation are strongly influenced by network

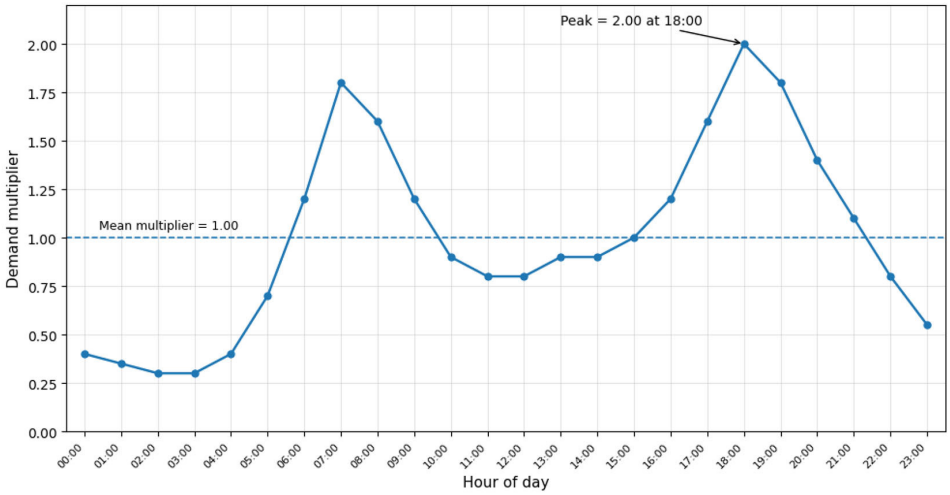

Figure 13. Normalized 24-hour design-sensitivity demand pattern applied in the extended-period hydraulic assessment

configuration and hydraulic conditions (Todini, 2000; Creaco et al., 2016). Therefore, identifying hydraulically sensitive locations provides valuable information for targeted monitoring and management strategies because it directs attention toward areas where changes in hydraulic conditions are most likely to influence service performance.

The results demonstrate the importance of evaluating resilience under multiple hydraulic scenarios rather than relying on a single design condition. While the network maintained acceptable performance under baseline and moderate demand increases, the peak-demand-equivalent scenario revealed reduced pressure margins at specific locations. This confirms that resilience assessment should consider both current hydraulic adequacy and the ability of gravity-based systems to tolerate future increases in hydraulic stress. By integrating scenario-based hydraulic evaluation with PSRI/PDI indicators, this study extends conventional hydraulic assessment by linking pressure sensitivity analysis with monitoring prioritization. The resulting framework supports system-specific monitoring strategies based on demonstrated hydraulic behaviour rather than generalized assumptions, providing a practical approach for improving resilience assessment of gravity-based water distribution networks.

Pipe failure vulnerability and critical component identification

Pipe failures create a fundamentally different hydraulic disturbance compared with gradual demand increases because they introduce localized changes in network connectivity, flow distribution, and pressure response. While increased demand progressively reduces available pressure margins across the system, individual component failures may produce abrupt hydraulic deterioration concentrated around affected locations. Previous resilience studies have emphasized that water distribution system performance depends not only on available hydraulic capacity but also on the ability of network topology and alternative flow pathways to maintain service following disturbances (Todini, 2000; Yazdani and Jeffrey, 2011). In this study, the pipe failure analysis complemented the demand-stress assessment by identifying components whose loss generated disproportionate changes in hydraulic performance.

The results demonstrate that hydraulic vulnerability is strongly influenced by the functional role of individual components within the network. Among the evaluated connected-network pipe outage scenarios, PIP-30 produced the largest hydraulic disturbance, demonstrating that component criticality depends on functional hydraulic importance rather than physical characteristics alone. The severe pressure reduction at J-34 and the associated increase in rerouted flow through PIP-2 show that failure of a hydraulically influential component can rapidly alter pressure distribution and create localized service degradation. Similar findings have been reported in water distribution reliability and resilience studies, where components with high hydraulic influence become critical because their failure can significantly alter flow distribution, pressure conditions, and serviceability (Walski et al., 2003; Yazdani & Jeffrey, 2011; Creaco et al., 2016).

The outage-specific PSRI further quantifies this distinction by showing that connected-network failures reduce pressure-service reliability to different degrees, with PIP-30 producing the greatest reduction among the evaluated connected-network outages.

The response of neighbouring pipes following failure provides additional information beyond pressure reduction alone. In this study, increased velocity in PIP-2 following PIP-30 removal demonstrated redistribution of hydraulic demand through alternative pathways. This confirms that failure sensitivity should be evaluated using multiple hydraulic indicators, since a component may reduce pressure directly while simultaneously increasing loading on remaining pipes. Therefore, combining pressure response, affected junctions, and flow redistribution provides a more complete representation of hydraulic vulnerability than relying on a single performance indicator.

The identification of bridge-link pipes provides an additional perspective on network resilience because their importance is associated with connectivity rather than only hydraulic performance under intact conditions. Removal of these links disconnects portions of the modeled system, demonstrating that some components contribute to resilience by maintaining available service pathways. Previous research has highlighted that network topology and connectivity characteristics strongly influence the ability of water distribution systems to tolerate failures and maintain functionality under disturbed conditions (Yazdani and Jeffrey, 2011; Creaco et al., 2016). Therefore, monitoring strategies should consider both

hydraulically sensitive components and topologically critical components.

The pipe failure analysis provides a direct foundation for the proposed monitoring strategy. Unlike demand-related stress, which generally produces progressive changes in pressure and loading conditions, localized failures generate distinct hydraulic signatures involving pressure decline, abnormal flow redistribution, and changes around the failed component. In this study, J-34, PIP-2, and PIP-30 were identified as complementary monitoring locations because they represent different aspects of failure response: pressure impact, redistribution behaviour, and component status. This demonstrates that hydraulic sensitivity analysis can translate failure simulations into practical monitoring priorities by linking specific hydraulic responses with measurable operational indicators.

Overall, the pipe failure analysis demonstrates that resilience of gravity-based water distribution networks depends not only on maintaining sufficient hydraulic head under increasing demand but also on preserving critical flow pathways during component disturbances. The identification of hydraulically influential pipes and connectivity-critical links provides a system-specific understanding of vulnerability that cannot be obtained from demand analysis alone. Integrating these findings with demand-based sensitivity results strengthens the proposed monitoring framework by enabling detection of both gradual hydraulic stress and localized failure-related disturbances.

Hydraulic sensitivity-based monitoring framework

Traditional hydraulic modelling is commonly used to evaluate network performance under specified operating conditions; however, translating hydraulic outputs into practical monitoring strategies remains a challenge. Monitoring systems based only on generalized sensor placement may generate extensive operational data without necessarily capturing locations where hydraulic changes become significant. In this study, hydraulic sensitivity analysis was used as a decision-support approach to identify monitoring locations and variables based on demonstrated network response under stressed conditions. The framework establishes a direct connection between resilience assessment and monitoring design by converting simulated hydraulic responses into targeted observation priorities.

The proposed framework was developed from the combined results of demand-loading and pipe-failure sensitivity analyses. Rather than selecting monitoring locations based only on physical characteristics or network size, locations were selected according to their demonstrated hydraulic response under changing operating conditions. This approach provides a system-specific basis for identifying where measurements are most informative.

Pressure monitoring represents the primary mechanism for detecting demand-related hydraulic stress. The identification of J-41 and J-116 as demand-sensitive junctions demonstrates that monitoring locations can be selected based on hydraulic sensitivity rather than uniform spatial distribution. Both locations experienced the largest pressure reductions under increased demand conditions and approached or exceeded the minimum service-pressure criterion under the peak-demand-equivalent condition. Therefore, these locations provide direct information on pressure-margin reduction under increasing hydraulic loading.

A major contribution of the framework is that abnormal conditions are interpreted using combined hydraulic signatures rather than a single measurement. Demand increases and localized pipe failures may both produce pressure reductions; however, their hydraulic responses differ. The framework therefore considers: pressure decline at demand-sensitive nodes as an indicator of demand-related stress, flow redistribution as an indicator of failure-related response, and asset-status information as confirmation for critical components.

This approach follows the monitoring logic developed in the Methods, where pressure, flow, velocity behaviour, and asset status were selected as complementary indicators.

Recent smart water management approaches increasingly integrate sensing technologies, IoT-enabled communication systems, and data-supported methods to improve infrastructure visibility and operational decision-making (Obunga et al., 2025; Silva et al., 2025). However, increasing data availability does not necessarily improve operational awareness unless measurements are connected with meaningful hydraulic behaviour and system-specific interpretation. Developments in IoT-based monitoring, digital decision-support systems, and digital-twin applications further highlight the importance of integrating

infrastructure models with operational information (Pagano et al., 2025; Chenevey and Cooper, 2026; Kim et al., 2026; Qureshi et al., 2026). The proposed framework complements these developments by providing a hydraulic sensitivity layer for selecting monitoring locations, measurable variables, and expected operational signatures.

The framework does not represent a fully deployed monitoring system; instead, it provides a hydraulic basis for selecting measurement locations, monitored variables, and abnormal-condition indicators. By establishing monitoring priorities from hydraulic evidence, the approach supports targeted data collection and improves interpretation of observed network behaviour.

The integration of hydraulic sensitivity analysis with monitoring design provides a practical pathway for improving operational awareness in gravity-based water distribution systems. The framework supports different monitoring objectives:

- J-41 and J-116 → demand-related pressure stress
- J-34 → localized outage response
- PIP-3 → conveyance loading condition
- PIP-2 → hydraulic redistribution
- PIP-30 and bridge links → critical asset condition

These selections are derived directly from simulated hydraulic behaviour rather than generalized assumptions. By integrating demand-stress analysis, pipe-failure vulnerability assessment, and temporal hydraulic response, the framework extends the role of hydraulic modelling from performance evaluation toward operational decision support. This approach aligns with emerging smart water management strategies that emphasize integration between infrastructure information, monitoring technologies, and decision-support processes (Ascenção et al., 2023).

Temporal hydraulic response and implications for resilient operation

Scenario-based resilience assessment provides valuable information about network behaviour under defined stress conditions; however, actual water distribution systems operate under continuously varying demand conditions. Therefore, an extended-period simulation (EPS) was conducted as a temporal validation step to evaluate whether sensitivity patterns identified from steady-state demand and outage scenarios remained representative during daily operation. The 24-hour hydraulic simulation complemented the steady-state resilience assessment by evaluating temporal variations in junction pressure, hydraulic response, and pipe-flow behaviour under time-varying demand conditions.

The temporal analysis demonstrates the operational relevance of the sensitivity-based monitoring approach. Monitoring strategies based only on extreme stress scenarios may not fully represent normal operating behaviour; therefore, sensitive locations should also be evaluated under changing daily conditions. The continued sensitivity of J-41 and J-116 during temporal simulation confirms their importance as pressure-monitoring locations because these junctions represent areas where available hydraulic margin changes significantly with demand variation. Their identification from both steady-state stress analysis and temporal response supports their selection as priority monitoring locations.

Daily demand variation creates a changing hydraulic operating envelope rather than a single fixed condition. Consequently, monitoring interpretation should consider whether observed hydraulic variables remain within the expected range established from model-based system behaviour. Higher-demand periods correspond to reduced pressure margins, while lower-demand periods allow recovery of hydraulic head. In addition, hydraulically sensitive downstream locations experience greater pressure variation than less vulnerable parts of the network. This approach allows measured values to be interpreted according to expected hydraulic behaviour rather than evaluated against a single fixed threshold.

The temporal response also provides insight into the behaviour of major conveyance components under changing operating conditions. Since PIP-3 was identified as the primary loading pathway during steady-state scenarios, its temporal flow and velocity response provide information regarding variation in system loading throughout the operating cycle. Similarly, redistribution-sensitive components such as PIP-2 can be evaluated through deviations from the normal hydraulic operating envelope, supporting differentiation between expected demand variation and abnormal hydraulic responses associated with localized disturbances.

By combining scenario-based stress response, pipe-failure sensitivity, and temporal hydraulic

variation, the proposed monitoring framework provides a more complete interpretation of network behaviour. Within this framework, J-41 and J-116 represent demand-related pressure sensitivity, J-34 represents localized disturbance response, PIP-3 represents changing conveyance loading, and PIP-2 represents abnormal redistribution behaviour. These relationships allow monitoring variables to be interpreted according to their expected hydraulic role within the system.

The temporal assessment therefore extends the application of hydraulic modelling from static performance evaluation toward continuous operational awareness. This perspective is particularly relevant in Jordan, where improving water-system efficiency and reducing operational burdens are important components of sustainable water-resource management strategies (Alwidyan et al., 2026). Integrating temporal analysis with scenario-based resilience assessment improves confidence in monitoring-location selection and supports the development of system-specific operational strategies for gravity-based water distribution networks.

Overall, the temporal hydraulic assessment demonstrates that resilience evaluation should consider both extreme stress conditions and normal operational variability. While scenario-based analysis identifies potential vulnerabilities, temporal simulation provides insight into how these vulnerabilities evolve during daily operation. The combination of both approaches provides a stronger basis for hydraulic sensitivity-based monitoring and resilient operation of gravity-based water distribution networks.

Limitations and future work

Several limitations should be considered. The hydraulic model was numerically verified against available WaterGEMS model outputs rather than calibrated or validated against field measurements; therefore, the proposed approach is intended for comparative hydraulic assessment and monitoring prioritization rather than direct prediction of real-time operating conditions. In addition, the analysis considered variable-demand conditions and single-pipe outage scenarios but did not include other sources of uncertainty, such as leakage development, valve operations, asset deterioration, or emergency operational responses.

Furthermore, the use of DDA means that severe pressure-deficient scenarios are interpreted as hydraulic sensitivity indicators rather than direct predictions of actual water availability. Future studies incorporating PDA formulations and field measurements could provide a more detailed assessment of pressure-dependent demand satisfaction and service continuity.

Accordingly, the temporal hydraulic envelopes proposed in this study should be regarded as pre-deployment, model-based reference ranges. Their transition toward operational monitoring would require field observations, consideration of sensor uncertainty, and characterization of actual system variability. Recent developments in Internet of Things (IoT)-based water-sector monitoring demonstrate the increasing potential of distributed sensing and connected monitoring technologies for supporting infrastructure assessment and operational decision-making (Obunga et al., 2025; Silva et al., 2025). Such field information could subsequently be used to calibrate the proposed hydraulic reference envelopes and establish site-specific operational alarm limits.

The present study is intentionally limited to the water-distribution network. Urban drainage systems involve distinct hydraulic and operational considerations (Butler et al., 2025), while wastewater-treatment systems introduce additional process-monitoring and optimization objectives, including emerging applications of artificial intelligence (Nagpal et al., 2024). These domains are therefore outside the scope of the present resilience and monitoring framework and should be addressed independently using methodologies appropriate to their respective hydraulic and process characteristics.

Future research should integrate field monitoring data with hydraulic model updating to evaluate the proposed framework under real operating conditions. Further development could incorporate IoT-enabled monitoring architectures and energy-aware sensing approaches (Obunga et al., 2025; Silva et al., 2025), together with digital-twin concepts that integrate physical infrastructure models, monitoring information, and operational decision support (Qureshi et al., 2026). Additional work should also consider uncertainty analysis, leakage scenarios, multi-component failures, and automated data-driven interpretation methods to strengthen real-time resilience assessment and operational decision support for gravity-based water distribution networks.

CONCLUSIONS

This study developed a scenario-based hydraulic resilience assessment approach integrated with a hydraulic sensitivity-based monitoring framework for a gravity-based water distribution network. The proposed approach combined validated hydraulic modelling, variable-demand scenario analysis, single-pipe outage assessment, pressure-based resilience indicators, and temporal hydraulic evaluation to identify critical hydraulic responses and translate them into system-specific monitoring priorities.

The study demonstrated that increasing hydraulic loading does not necessarily produce uniform degradation throughout a water distribution network. Instead, pressure limitations emerge at specific hydraulically sensitive locations where available pressure margins become reduced under stressed conditions. Similarly, single-pipe outage analysis showed that component importance is governed not only by physical characteristics but also by hydraulic influence and network connectivity, with certain components producing disproportionate changes in system performance when unavailable. These findings highlight the importance of evaluating both demand-related stress and component-related disturbances when assessing resilience in gravity-based systems.

The main scientific contribution of this study is the integration of hydraulic sensitivity analysis with monitoring framework development. Rather than using hydraulic modelling only to evaluate system performance under predefined operating conditions, the proposed approach converts model-based sensitivity results into monitoring information by identifying priority locations, measurable variables, and expected hydraulic response signatures. The integration of pressure-based resilience indicators, including the pressure service reliability index (PSRI) and pressure degradation index (PDI), further improves interpretation of resilience changes by distinguishing overall pressure-service reliability from localized pressure deterioration.

From a practical perspective, the proposed approach provides a systematic basis for supporting monitoring design in gravity-based water distribution systems. By prioritizing hydraulically sensitive junctions, influential pipe sections, and connectivity-critical components, monitoring resources can be directed toward locations where changes in hydraulic behaviour provide the most informative indication of demand stress or localized disturbances. This supports more targeted operational awareness compared with monitoring strategies based only on generalized network characteristics.

Acknowledgments

The authors gratefully acknowledge the support of the Deanship of Scientific Research at Amman Arab University, which facilitated the research and modelling work conducted at the College of Engineering.

REFERENCES

1. Alwidyan, M., Jaradat, A., Ahmad, O., Al Assaf, A. (2026). Optimizing water and energy efficiency in jordan: challenges, opportunities, and sustainable solutions for the future. *Jordan Journal of Mechanical and Industrial Engineering 20*(1), 97–113. https://doi.org/10.59038/jjmie/200109
2. Ascenção, É. S., Almeida, C. F. M., Kagan, N. (2023). Integration model for smart water management systems: A systematic literature review. In *2023 15th IEEE International Conference on Industry Applications (INDUSCON)* (pp. 1178–1184). Institute of Electrical and Electronics Engineers. https://doi.org/10.1109/INDUSCON58041.2023.10375038
3. Bai, Y., Geng, B., Yan, H., Tao, T., Hao, J., Xin, K. (2026). Building smart urban water systems from source to tap: Applications and challenges of deep learning. *Journal of Water Process Engineering, 82*, 109420. https://doi.org/10.1016/j.jwpe.2025.109420
4. Butler, D., Digman, C., Makropoulos, C., Davies, J. W. (2025). *Urban drainage* (5th ed.). CRC Press. https://doi.org/10.1201/9781003408635
5. Chenevey, B., Cooper, J. (2026). Model or digital twin? AWWA survey on water distribution technology. *Journal AWWA, 118*, 36–45. https://doi.org/10.1002/awwa.70075
6. Creaco, E., Franchini, M., Todini, E. (2016). The combined use of resilience and loop diameter uniformity as a good indirect measure of network reliability. *Urban Water Journal, 13*(2), 167–181. https://doi.org/10.1080/1573062X.2014.949799
7. Di Nardo, A., Boccelli, D. L., Herrera, M., Creaco, E., Cominola, A., Sitzenfrei, R., Taormina, R. (2021). Smart urban water networks: Solutions, trends and challenges. *Water, 13*(4), 501. https://doi.org/10.3390/w13040501
8. Fasha, M., Al-Maayta, N., Sowan, B., Athamneh, M., Barham, H. (2026). AI-driven framework for

adaptive water network management with proof-of-concept implementation: Addressing non-revenue water in Jordan. *arXiv*. https://arxiv.org/abs/2606.15709

9. Jayaram, N., Srinivasan, K. (2008). Performance-based optimal design and rehabilitation of water distribution networks using life cycle costing. *Water Resources Research, 44*(1), W01417. https://doi.org/10.1029/2006WR005316
10. Joseph, K., Sharma, A. K., Van Staden, R. (2022). Development of an intelligent urban water network system. *Water, 14*(9), 1320. https://doi.org/10.3390/w14091320
11. Kim, Y., Huang, Y., Cantrell, R., Bartos, M., Sela, L. (2026). From field data to smart operations: A digital twin framework for water distribution systems in remote communities. *ACS ES&T Water, 6*(6), 3543–3554. https://doi.org/10.1021/acsestwater.5c01515
12. Krishnan, S. R., Nallakaruppan, M. K., Chengoden, R., Koppu, S., Iyapparaja, M., Sadhasivam, J., Sethuraman, S. (2022). Smart water resource management using artificial intelligence: A review. *Sustainability, 14*(20), 13384. https://doi.org/10.3390/su142013384
13. Maroju, R. G., Choudhari, S. G., Shaikh M., et al. (2023). Application of Artificial Intelligence in the Management of Drinking Water: A Narrative Review. *Cureus 15*(11), e49344. https://doi.org/10.7759/cureus.49344
14. Nagpal, M., Siddique, M. A., Sharma, K., Sharma, N., Mittal, A. (2024). Optimizing wastewater treatment through artificial intelligence: Recent advances and future prospects. *Water Science & Technology, 90*(3), 731–757. https://doi.org/10.2166/wst.2024.259
15. Obunga, P. O., Rwanga, S. S., Dinka, M. O., Otieno, B. O. (2025). Review of the emerging technologies in the water sector with a focus on the deployment of Internet of Things solutions. *npj Clean Water, 8*, Article 53. https://doi.org/10.1038/s41545-025-00487-x
16. Pagano, A., Garlisi, D., Giuliano, F., Cattai, T., Cuomo, F. (2024). SWI-FEED: Smart water IoT framework for evaluation of energy and data in massive scenarios. *arXiv*. https://doi.org/10.48550/arXiv.2404.07692
17. Pagano, A., Garlisi, D., Tinnirello, I., Giuliano, F., Garbo, G., Falco, M., Cuomo, F. (2025). A survey on massive IoT for water distribution systems: Challenges, simulation tools, and guidelines for large-scale deployment. *Ad Hoc Networks, 168*, 103714. https://doi.org/10.1016/j.adhoc.2024.103714
18. Prasad, T. D., Park, N. (2004). Multiobjective genetic algorithms for design of water distribution networks. *Journal of Water Resources Planning and Management, 130*(1), 73–82. https://doi.org/10.1061/(ASCE)0733-9496(2004)130:1(73)
19. Qureshi, M., Feng, Z., Kumar, V., Besharat, M., Lovreglio, R. (2026). A systematic literature review of digital twin applications for sustainable water systems in natural and built environment. *Discover Sustainability*. https://doi.org/10.1007/s43621-026-03825-2
20. Rossman, L. A. (2022). *EPANET 2.2 user manual* (EPA/600/R-22/144). U.S. Environmental Protection Agency. https://www.epa.gov/water-research/epanet
21. Silva, J. B., Oliveira, R., Ferreira, L., Santos, F. (2025). Smart water management: An energetically autonomous IoT-based monitoring approach. *Sensors, 25*(23), 7227. https://doi.org/10.3390/s25237227
22. Suribabu, C. R. (2017). Resilience-based optimal design of water distribution network. *Applied Water Science, 7*, 4055–4066. https://doi.org/10.1007/s13201-017-0560-2
23. Todini, E. (2000). Looped water distribution networks design using a resilience index based heuristic approach. *Urban Water, 2*(2), 115–122. https://doi.org/10.1016/S1462-0758(00)00049-2
24. Walski, T. M., Chase, D. V., Savic, D. A., Grayman, W., Beckwith, S., Koelle, E. (2003). Advanced water distribution modeling and management. Haestad Press.
25. Yazdani, A., Jeffrey, P. (2011). Resilience enhancing expansion strategies for water distribution networks. *Environmental Modelling & Software, 26*(12), 1574–1585. https://doi.org/10.1016/j.envsoft.2011.07.016